Journal of Shahrekord University of Medical Sciences
doi: 10.34172/jsums.1038 2025;27(3):126-133 http://j.skums.ac.ir

Original Article

Assessment of Antibacterial Efficacy of Silver Oxide Nanoparticles and *Lactobacillus casei* Against the Clinical Isolates of *Acinetobacter baumannii*

Wisam Talib-Ali[1], **Ashraf Kariminik**[2,3*], **Atousa Ferdousi**[4]

[1]Department of Microbiology, SR.C., Islamic Azad University, Tehran, Iran
[2]Department of Microbiology, Ker.C. Islamic Azad University, Kerman, Iran
[3]Food and Agricultural Safety Research Center, Ker.C., Islamic Azad University, Kerman, Iran
[4]Department of Microbiology, ShQ.C., Islamic Azad University, Tehran, Iran

*Corresponding Author: Ashraf Kariminik, Email: a.kariminik@iauk.ac.ir

Abstract

Background and aims: *Acinetobacter baumannii* is recognized as a multidrug-resistant pathogen, notably associated with biofilm formation and antibiotic resistance in healthcare environments. The rising incidence of infections attributable to this organism highlights the urgent necessity for alternative therapeutic approaches. This study aimed to assess the antibacterial efficacy and antibiofilm activity of silver oxide nanoparticles and *Lactobacillus casei* against clinical isolates of *A. baumannii*.

Methods: Overall, 150 *A. baumannii* isolates were collected from urine samples in Tehran, Iran, ensuring 80% statistical power and a 95% confidence level. The isolates were categorized by resistance profiles and treated with Ag NPs, *L. casei* supernatant, and their combination. Ag NPs were biosynthesized using *L. casei* extracts and characterized by scanning electron microscopy, energy dispersive X-ray spectroscopy, and Fourier transform infrared spectroscopy. Antibacterial and antibiofilm effects were assessed using broth microdilution and microtiter assays. Finally, the analysis of variance and t-test were conducted in SPSS 26 ($P<0.05$).

Results: Based on the results, 18 isolates exhibited high resistance to β-lactam antibiotics and fluoroquinolones. Ag NPs (40 µg/mL) resulted in a 93.04% reduction in bacterial growth, while *L. casei* supernatant showed a 76.45% decrease. The combination of Ag NPs and *L. casei* supernatant demonstrated strong synergistic effects, achieving a 98.24% reduction in bacterial growth. Antibiofilm assays revealed a significant 95.3% inhibition of biofilm formation with the combination therapy ($P<0.001$).

Conclusion: This study highlights the potential of combining Ag NPs and probiotic-derived compounds as a novel approach to combat multidrug-resistant *A. baumannii*. These findings suggest promising avenues for enhancing antimicrobial therapies and addressing the challenge of antibiotic resistance in clinical settings.

Keywords: Silver oxide nanoparticles, *Lactobacillus casei*, *Acinetobacter baumannii*, Synergism

Received: December 27, 2024, **Revised:** March 10, 2025, **Accepted:** March 10, 2025, **ePublished:** September 8, 2025

Introduction

Acinetobacter is a genus of bacteria that includes several species, with *Acinetobacter baumannii* being the most clinically significant. This bacterium has emerged as a major opportunistic pathogen, particularly in healthcare settings (1). It is known for causing various infections, especially in immunocompromised patients or those with prolonged hospital stays (2). Biofilms are structured communities of bacteria that adhere to surfaces and are embedded in a self-produced extracellular matrix. *A. baumannii* is particularly adept at forming biofilms on medical devices, such as catheters and ventilators, as well as on tissues within the human body (3). The biofilm provides a protective environment for the bacteria, making them more resistant to the host immune response and antimicrobial agents. One of the most concerning aspects of *Acinetobacter* is its high level of antibiotic resistance (3). *Acinetobacter* species possess inherent resistance mechanisms, such as the ability to efflux antibiotics and the low permeability of their outer membrane, limiting the entry of many drugs. *A. baumannii* can acquire resistance genes through horizontal gene transfer, often from other bacteria (4), including genes that confer resistance to different classes of antibiotics (5). In addition, the biofilm matrix can impede the penetration of antibiotics, making it difficult for these drugs to reach adequate concentrations at the site of infection (6). Thus, some *Acinetobacter* cells can enter a dormant state within biofilms, making them less susceptible to antibiotics (7). The combination of biofilm formation and antibiotic resistance makes *A. baumannii* a formidable pathogen in healthcare settings (8). Effective management strategies include *Lactobacillus casei*, a beneficial bacterium that resides in the human gut and is also used as a probiotic. Various studies suggest that *L. casei* may possess antimicrobial properties, which could play a role in preventing certain infections (9). Silver oxide nanoparticles (AgO NPs) have been found

to exhibit potent antibacterial properties (10). The antibacterial properties of AgO NPs are primarily due to their tiny dimensions, which allow them to breach bacterial cell walls and membranes, disrupting critical cellular functions. After penetrating the bacterial cell, NPs can engage with proteins and enzymes, ultimately causing cell death (11, 12). Ag NPs have been reported to exhibit antimicrobial activity against *Acinetobacter* by disrupting the bacterial cell membrane. In contrast, *Lactobacillus* species have been shown to inhibit the growth of *Acinetobacter* by producing antimicrobial compounds and competing for nutrients (13, 14). Overall, using Ag NPs and *Lactobacillus* species against *Acinetobacter* offers a promising approach to combat antibiotic-resistant infections, potentially reducing the risk of treatment failure and improving patient outcomes. This study aims to identify the effect of a combination of AgO NPs and *L. casei* supernatant on clinical drug-resistant *A. baumannii* isolates.

Materials and Methods

Isolation and Identification of Bacteria

One hundred fifty urine samples were obtained from patients suspected of having urinary tract infections (UTIs) at several healthcare centers in Tehran, Iran, from December 2023 to March 2024. The samples were collected from individuals exhibiting common UTI symptoms, including dysuria, frequent urination, urgency, or flank pain. Patients who had received antibiotic treatment for a UTI within the past 48 hours were excluded from the study to prevent any impact on bacterial growth. Urine samples were collected using the clean-catch midstream technique to minimize contamination from the external genital area. All patients provided informed consent before sample collection. The samples were collected in sterile containers, ensuring minimal contamination during the process. The sampling method included demographic stratification by age groups, focusing on high-risk populations, such as older adults. The collected urine samples were transported to the laboratory within 2 hours after collection to prevent bacterial overgrowth or loss of viability. Each urine sample (10 µL) was inoculated onto blood agar and MacConkey agar plates using a sterile calibrated loop. The plates were incubated at 37°C for 24 hours under aerobic conditions. Following incubation, the number of colonies was counted, and the growth was categorized according to colony morphology and Gram staining. Significant bacterial growth (≥10^5 CFU/mL) indicated infection. Isolates showing significant growth on both media were further identified based on their colony morphology, Gram stain, and biochemical reactions. Biochemical testing encompassing catalase and oxidase and specific tests (e.g., Simmons Citrate, triple sugar iron, urease, and Methyl Red/Voges-Proskauer) were used (15). All culture media were sourced from Merck, Germany. Additionally, molecular methods, including the polymerase chain reaction (PCR) amplification of the *recA* gene, were utilized to confirm the identity of *A. baumannii* isolates. According to the manufacturer's instructions, DNA was extracted from bacterial colonies with a commercial DNA extraction kit (Karmania Pars Gene, Iran). The *recA* gene was amplified with specific primers F 5′-CCTGAATCTTCTGGTAAAAC-3' and R 5′-GTTTCTGGGCTGCCAAACATTAC-3' for the confirmation of *A. baumannii* (16). The PCR for each gene was performed in a volume of 20 µL. The PCR temperature program for all genes included: initial denaturation at 95°C for 5 minutes, 35 cycles of denaturation at 95°C for 40 seconds, annealing at 57.5°C for 1 minute, and extension at 72°C for 2 minutes, and final extension at 72°C for 5 minutes. The amplified gene fragments using this technique were visualized by 1% agarose gel electrophoresis alongside a 100 bp ladder. The sample size was estimated based on the expected prevalence rates of multidrug-resistant *A. baumannii* in clinical settings. Statistical power was set at 80%, and a confidence level of 95% was targeted.

Antibiotic Resistance Pattern Test

In the current study, a disc diffusion susceptibility test was performed on Mueller-Hinton agar (Merck, Germany) based on Clinical and Laboratory Standards Institute documents to determine the susceptibility of isolated bacteria (17). The antibiotic discs (Padtan Teb, Iran) were ceftriaxone (30 µg), aztreonam (30 µg), ciprofloxacin (5 µg), levofloxacin (5 µg), piperacillin-tazobactam (30 µg), meropenem (10 µg), imipenem (10 µg), amikacin (30 µg), gentamicin (10 µg), tetracycline (30 µg), tigecycline (10 µg), and polymyxin B (10 µg).

Preparation of Lactobacillus and Supernatant Extraction

L. casei PTCC 1608 was cultivated in de Man, Rogosa, and Sharpe (MRS) broth (Merck, Germany) for 48 hours at 37°C in a microaerophilic condition to reach the stationary phase. Afterward, the culture was centrifuged for 30 minutes at 1500 × g to collect the supernatant. This supernatant was then filtered using a 0.22-µm filter and neutralized with an acid and catalase enzyme (18).

Biosynthesis of Silver Oxide Nanoparticles

L. casei PTCC 1608 was grown in MRS broth (Merck, Germany) at 37°C for 24 hours. The bacterial culture was then centrifuged at 10,000 rpm for 10 minutes to obtain the pellet, which was washed twice with sterile distilled water. A 1 mM Ag nitrate (Merck, Germany) solution was prepared by dissolving Ag nitrate in sterile distilled water. This solution was filtered through a 0.22 µm filter (Millipore, Merck, Germany) to remove contaminants. The washed *Lactobacillus* pellet was added to the 1 mM Ag nitrate solution (typically a 1:10 ratio of bacterial suspension to the Ag nitrate solution). The mixture was incubated at 37°C for 48 hours under continuous shaking at 150 rpm to allow the biosynthesis of AgO NPs. The formation of NPs was observed by the color change

from colorless to brown, indicating the reduction of Ag ions to Ag NPs (19). NPs were characterized by scanning electron microscopy (SEM), energy dispersive X-ray spectroscopy (EDS/EDX), and Fourier transform infrared spectroscopy (FTIR).

Antibacterial Effects of Silver Nanoparticles and Lactobacillus Casei

Appropriate concentrations of Ag NPs (0 µg/mL, 1.25 µg/mL, 2.5 µg/mL, 5 µg/mL, 10 µg/mL, 20 µg/mL, and 40 µg/mL) were prepared for use in the experiments. *L. casei* were cultured in the MRS broth and incubated at 30°C for 24 hours. After incubation, the bacterial culture was centrifuged at a specific revolution per minute and duration to collect the supernatant. The supernatant was filtered through a 0.22 µm membrane to remove bacterial cells and stored at 4°C until use. *Acinetobacter* isolates (S9 and S14) were used, and bacterial isolates were cultured in the lysogeny broth before being used in susceptibility testing. The broth microdilution method was used to evaluate the antimicrobial effects of AgO NPs and the *Lactobacillus* supernatant on *Acinetobacter* isolates. A 96-well µL plate was prepared with varying concentrations of AgO NPs (0–40 µg/mL) and a fixed volume of the *Lactobacillus* supernatant. Wells containing only bacterial inoculum and growth medium served as negative controls. In contrast, a known antibiotic served as a positive control. Each well was inoculated with 100 µL of a standardized bacterial suspension (1×10^6 CFU/mL). Wells were supplemented with 100 µL of AgO NPs or the *Lactobacillus* supernatant, alone or in combination. The plates were incubated at 37°C for 24 hours. A microplate reader assessed bacterial growth by measuring optical density (OD) at 600 nm. The percentage inhibition of bacterial growth was calculated as inhibition (%) = (1−OD test/OD control) × 100. All experiments were performed in triplicate (20).

Biofilm Formation and Inhibition Assay

The antibiofilm activity of AgO NPs and the *Lactobacillus* supernatant, alone or in combination, was assessed using a 96-well microtiter plate assay. Each microtiter plate well was inoculated with 100 µL of bacterial suspension (1×10^8 CFU/mL)—wells containing 100 µL of growth medium without bacteria served as negative controls. AgO NPs (1.25–40 mg/mL), the *Lactobacillus* supernatant, or their combination were added to the respective wells. Untreated wells with bacterial suspension served as positive controls. The plates were incubated at 37°C for 24 hours to allow biofilm formation. After incubation, wells were gently washed three times with phosphate-buffered saline to remove planktonic bacteria. Biofilms were fixed with methanol (Digishimi, Iran) for 15 minutes and stained with 0.1% crystal violet (Merck, Germany) for 15 minutes. Excess dye was removed by washing with phosphate-buffered saline, and the dye bound to biofilm was solubilized with 33% acetic acid. Each well's OD was measured at 570 nm using a microplate reader. The percentage inhibition of biofilm formation was calculated using the following formula:

Biofilm inhibition (%) = (1−OD test/OD control) × 100 (21).

Statistical Analysis

Data were analyzed using SPSS, version 26. Descriptive statistics (means ± standard deviations) were used to summarize data, and inferential statistics (analysis of variance and t-tests) were applied for group comparisons. $P < 0.05$ was considered statistically significant.

Results

In general, 18 *A. baumannii* samples were isolated and identified based on phenotypic and molecular investigations. No isolates were observed in individuals aged 1–30 years. The highest percentage of isolates (50%) was found in individuals aged 61–75, highlighting older adults as the most affected group. The 41–50-year-old and 51–60-year-old groups accounted for 22.22% and 16.66% of cases, respectively. The mean (±SD) age of affected individuals was 58.7 (±12.4) years, emphasizing an age-related susceptibility to *A. baumannii* infections. These results indicated a significant representation of middle-aged adults among the affected population. A relatively low percentage of isolates (11.12%) was reported in the 31–40-year-old group, suggesting lesser susceptibility than in older age groups. The frequency distribution of *A. baumannii* isolates indicates a clear trend of age-related susceptibility, with most infections occurring in individuals aged 61–75 years old. This underscores the need for enhanced infection control measures and targeted care in older populations to mitigate the risk of *A. baumannii* infections. Middle-aged adults also represent a notable at-risk group, emphasizing the importance of broader preventive strategies.

Determination of Antibiotic Sensitivity in Isolated Bacteria

Based on the results, in the case of piperacillin-tazobactam, no strains were sensitive; overall, 50% were intermediate, and 50% were resistant, indicating significant resistance. Ciprofloxacin and tigecycline showed high resistance (33.33% and 16.66%, respectively) and intermediate response (55.55% and 77.77%). Tetracycline represented 61.11% intermediate response with 16.66% resistance, demonstrating moderate efficacy. Most strains were sensitive to aztreonam and gentamicin (77.77%), making them the most effective antibiotics in this study. In addition, 50% sensitivity to amikacin suggests that it is a relatively effective option against *A. baumannii*. Polymyxin B revealed sensitivity in 44.44% of strains, indicating its potential for treatment but not as a first-line option. Meropenem and imipenem, both carbapenems, displayed significant intermediate responses (55.55% and

77.77%, respectively), though resistance was observable (5.55% and 22.22%). Ceftriaxone and levofloxacin illustrated low sensitivity (5.55%) and high intermediate response (66.66% and 77.77%), with notable resistance to ceftriaxone (27.77%). Accordingly, *A. baumannii* isolates exhibited multidrug resistance, particularly against β-lactam/β-lactamase inhibitors (e.g., piperacillin-tazobactam) and fluoroquinolones (e.g., ciprofloxacin and levofloxacin).

Characterization of Biosynthesized Silver Oxide Nanoparticles

Figure 1 depicts an SEM image of AgO NPs with varying sizes (ranging from approximately 9 nm to 60 nm in size), indicating polydispersity in particle size. The NPs had irregular shapes, some showing spherical and aggregated forms. The observed clusters might be due to agglomeration, a common phenomenon in NPs due to their high surface energy. The NPs have relatively smooth surfaces, but some roughness or uneven structures are also evident. Smaller NPs (e.g., L3) may be observed on or near larger aggregates, representing hierarchical growth or clustering during synthesis. The magnification used in this SEM image was 250 kx (250,000 times), which provides a highly detailed view of the surfaces of NPs. The scale bar indicates 200 nm, giving an apparent spatial reference for the size of the NPs. Figure 2 displays an EDS/EDX analysis of AgO NPs. Multiple strong peaks at characteristic energy levels (around 2.98 keV and higher) confirmed the presence of Ag as a primary component in NPs. The most intense peaks belonged to Ag, affirming that Ag was the dominant element in the analyzed sample. This is consistent with the synthesis of AgO NPs. Figure 3 illustrates an FTIR spectrum of AgO NPs, which was used to identify functional groups, chemical bonds, and surface capping agents in synthesized NPs. The peak at ~3271 cm^{-1} corresponds to the stretching vibration of the hydroxyl group (-OH), which may originate from water molecules or hydroxyl groups on the surface of NPs, demonstrating the presence of moisture or capping agents with hydroxyl functionalities used during NP synthesis. The peak at ~2121 cm^{-1} could be associated with the stretching vibrations of C≡C (alkyne) or C≡N (nitrile) bonds. It may represent organic molecules or residual precursors used in the biosynthesis process. The peak at ~1615 cm^{-1} is characteristic of carbonyl (C=O) stretching vibrations or aromatic C=C bonds. It could indicate the presence of biomolecules, such as proteins or enzymes, utilized to reduce or stabilize AgO NPs. The peak at ~598 cm^{-1} is likely related to Ag–O stretching vibrations, confirming the formation of AgO NPs.

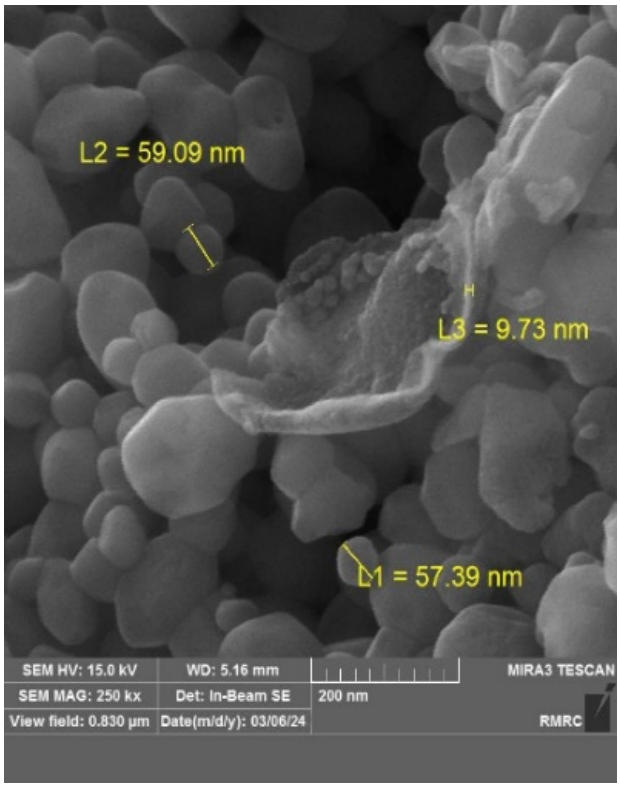

Figure 1. SEM Image of AgO Nanoparticles
Note. AgO: Silver oxide; SEM: Scanning electron microscopy

Synergistic Activity

The extract of *Lactobacillus* and Ag NPs, each alone, had antibacterial effects on 2 antibiotic-resistant isolates of *A. baumannii* (Table 1). Regarding isolate S9, Ag NPs (at 40 mg/µL and 20 mg/µL) showed a growth reduction of 93.04% and 83.77%, respectively. For isolate S14, Ag NPs demonstrated a growth reduction of 88.45% and 84.88% at the same concentrations after 24 hours. In the case of isolate S9, the supernatant of *Lactobacillus* (at 40 mg/µL and 20 mg/µL) represented a growth reduction of 70.35% and 56.52%, respectively. Concerning isolate S14, at the

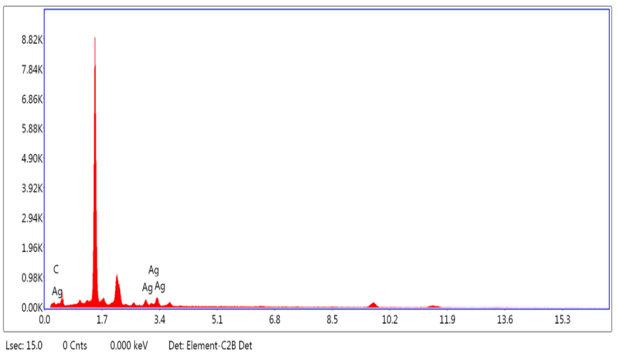

Figure 2. Energy Dispersive X-Ray Spectroscopy of AgO Nanoparticles
Note. AgO: Silver oxide

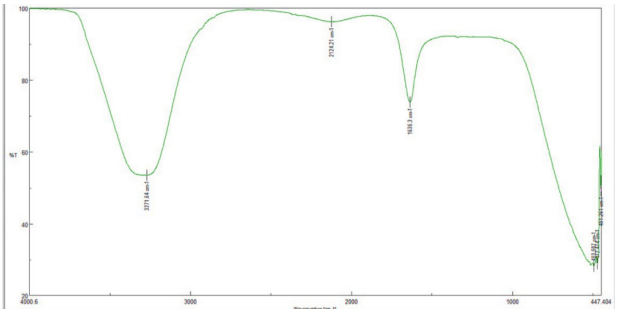

Figure 3. FTIR Analysis of AgO Nanoparticles
Note. FTIR: Fourier transform infrared spectroscopy; AgO: Silver oxide

Table 1. Antibacterial and Synergistic Effects of *L. casei* and Silver Nanoparticles Against Two Resistant Isolates of *A. baumannii*

Variables							
	Ag Nanoparticle Treatment						
Concentration (µg/mL (	*0	1.25	2.5	5	10	20	40
	0.64	0.666	0.324	0.312	0.284	0.105	0.045
Bacterial isolate S9 Growth decrease after 24 hours (%)	-	0.29 ± 0.66	49.92 ± 0.32	51.77 ± 0.31	56.10 ± 0.28	83.77 ± 0.10	93.04 ± 0.04
Bacterial isolate S14	0.87	0.789	0.608	0.574	o.311	0.133	0.101
Growth decrease after 24 hours (%)	-	9.69 ± 0.78	30.43 ± 0.60	34.32 ± 0.57	64.42 ± 0.31	84.88 ± 0.13	88.45 ± 0.10
	***Lactobacillus* Treatment**						
Bacterial isolate S9	0.61	0.600	0.555	0.497	0.382	0.267	0.182
Growth decrease after 24 hours (%)	-	2.28 ± 0.60	9.61 ± 0.55	19.06 ± 0.49	37.79 ± 0.38	56.52 ± 0.26	70.35 ± 0.18
Bacterial isolate S14	0.65	0.702	0.621	0.412	0.371	0.203	0.154
Growth decrease after 24 hours (%)	-	7.33 ± 0.70	5.05 ± 0.62	37.00 ± 0.41	43.28 ± 0.37	68.97 ± 0.20	76.45 ± 0.15
	***Lactobacillus* and Ag Nanoparticle Treatment**						
Bacterial isolate S9	0.96	0.819	0.662	0.401	0.209	0.097	0.017
Growth decrease after 24 hours (%)	-	15.31 ± 0.81	31.54 ± 0.66	58.54 ± 0.40	78.3 ± 0.20	95.30 ± 0.09	98.24 ± 0.01
Bacterial isolate S14	0.86	0.833	0.517	0.473	0.333	0.197	0.087
Growth decrease after 24 hours (%)	-	3.48 ± 0.83	40.09 ± 0.51	45.19 ± 0.47	61.41 ± 0.33	90.91 ± 0.19	97.17 ± 0.08

Note. Ag: Silver; *L. casei*: *Lactobacillus casei*; *A. baumannii*: *Acinetobacter baumannii*.

same concentrations, the supernatant of *Lactobacillus* exhibited a growth reduction of 76.45% and 68.97% after 24 hours. As regards isolate S9, the combination of Ag NPs and the supernatant of *Lactobacillus* (at 40 mg/µL and 20 mg/µL) revealed a growth reduction of 98.24% and 95.30%, respectively. For isolate S14, the combination of *Lactobacillus* and Ag NPs resulted in a growth reduction of 90.91% and 97.17% at the same concentrations after 24 hours. Antibacterial activity tests confirmed that Ag NPs could reduce bacterial growth by 93.04% (mean ± SD: 92.6 ± 0.3%) at 40 µg/mL, while the *L. casei* supernatant showed a 76.45% reduction (mean ± SD: 75.8 ± 0.5%). The combination treatment achieved a significant 98.24% reduction (mean ± SD: 97.9 ± 0.4%). Antibiofilm assays demonstrated synergistic effects, with biofilm inhibition rates significantly higher for the combination treatment ($P < 0.001$). When treated with Ag NPs, a substantial reduction in growth was observed in Isolate S9 (e.g., a 93.04% decrease at 40 mg/µL) and Isolate S14 (e.g., an 88.45% decrease at 40 mg/µL). The reduction in growth diminished with decreasing concentrations, indicating a concentration-dependent effect. For *Lactobacillus* treatment, moderate growth inhibition was noted in Isolates S9 (70.35% reduction at 40 mg/µL) and S14 (76.45% reduction at 40 mg/µL). These effects were less pronounced compared to Ag NPs. However, when the treatments were combined, the inhibitory effects were maximized, suggesting a synergistic interaction, particularly at higher concentrations. The minimum inhibitory concentration value for the combination of *Lactobacillus* and Ag NPs was 40 mg/mL, achieving over 90% growth inhibition.

Assessment of Antibiofilm Activity

The microtiter plate method was employed to investigate the antibiofilm effects of biosynthesized Ag NPs and the *L. casei* supernatant. The results of the anti-biofilm effects indicated that although Ag NPs alone can significantly reduce biofilm formation and effectively prevent cell binding, significant synergistic effects were observed in preventing binding compared to the effects of supernatant and in the form of a combination of both active ingredients. Figure 3 displays the anti-biofilm activity of AgO NPs, the supernatant *Lactobacillus*, and the combination of AgO NPs and the supernatant against biofilm formation, measured as OD at 570 nm at various concentrations (1.25–40 mg/µL). The control group (blue bar) shows the highest OD value, indicating robust biofilm formation without any treatment. AgO NPs alone (purple bars) display a concentration-dependent reduction in biofilm formation. The OD decreased as the concentration increased from 1.25 mg/µL to 40 mg/µL, highlighting enhanced biofilm inhibition. At 40 mg/µL, AgO NPs achieved significant biofilm inhibition, but biofilm persisted to some extent. The supernatant alone (green bars) depicts moderate biofilm inhibition compared to the control, with noticeable reductions at higher concentrations (e.g., 20 mg/µL and 40 mg/µL). However, its anti-biofilm activity was less pronounced than that of AgO NPs. The combination (yellow bars) demonstrated the most potent biofilm inhibition, with the OD values significantly lower than those observed for either AgO NPs or the supernatant alone at all tested concentrations. The combination effect was particularly evident at 20 mg/µL and 40 mg/µL, where the biofilm formation is almost entirely inhibited (very low OD values), indicating a synergistic effect. Figure 4 illustrates the antibiofilm effects of Ag NPs, *L. casei* supernatant, and their combination. A statistically significant reduction in biofilm formation was observed with the combination treatment compared to individual components ($P < 0.001$). Data are presented as means ± SDs at multiple concentrations. AgO NPs revealed

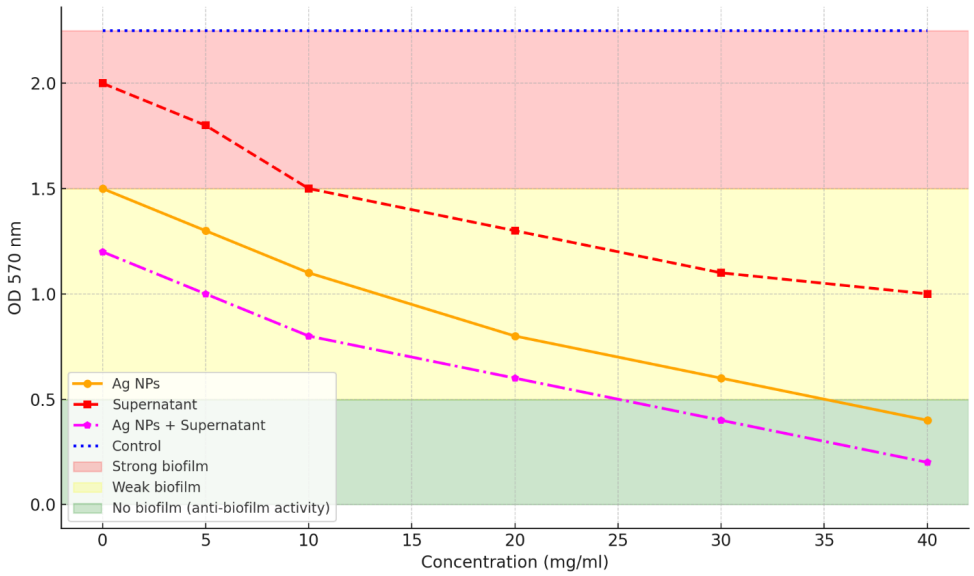

Figure 4. Anti-Biofilm Effects of Biosynthesized Silver Nanoparticles and *L. casei* Supernatant on *A. baumannii*
Note. Ag NP: Silver nanoparticles; *L. casei*: *Lactobacillus casei; A. baumannii*: *Acinetobacter baumannii*

significant reductions in OD values with increasing concentrations. The combination of AgO NPs and the supernatant had the most pronounced effects, similar to the trends observed in Table 1. The standalone supernatant effect (likely equivalent to *Lactobacillus* treatment) was moderate, supporting the comparative outcomes (Table 1). Table 1 presents the percentage reduction in bacterial growth after 24 hours of treatment exposure. Ag NPs consistently showed superior performance compared to the *Lactobacillus* extract, and the combined treatment of both agents resulted in the most significant growth reduction for both isolates. Figure 4, which depicts biofilm inhibition, likely supports the conclusion that Ag NPs play an important role in disrupting biofilm formation, with additional benefits provided by the *L. casei* supernatant. There was a synergistic effect when both *Lactobacillus* and Ag NPs were used together (Table 1), as the growth reductions for both isolates (S9 and S14) were considerably more significant in the combined treatment group. This suggests that combining the two treatments enhances their antibacterial and anti-biofilm properties. Figure 4 confirms this issue by illustrating a more substantial reduction in biofilm formation in the combined treatment compared to individual treatments. This observation aligns with the growth reduction data from Table 1 and further underscores the enhanced effectiveness of the combined treatment. Table 1 and Figure 4 offer valuable insights into the synergistic interaction between the *Lactobacillus* extract and Ag NPs in fighting *A. baumannii*. While Table 1 provides quantitative evidence of the superior effectiveness of the combination treatment in reducing bacterial growth, Figure 4 likely highlights similar trends, emphasizing the combination's enhanced ability to combat biofilm formation, a crucial factor in treating infections caused by resistant strains, such as *A. baumannii*. Based on the results (Figure 5), the strong biofilm (dark blue) suggests a high concentration

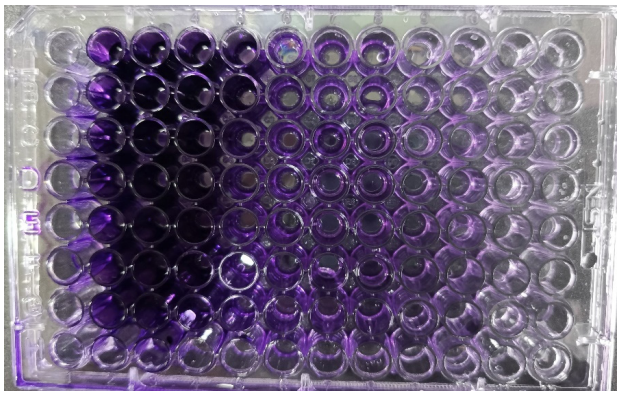

Figure 5. Microtiter Plate Assay Showing the *Strong, **Weak, and ***No Biofilm
Note. *Dark blue, **light blue, and ***transparent

of adhered cells and extracellular polymeric substances. The weak biofilm (bright blue) indicates some adherence but lower biomass or extracellular polymeric substances production, and the absence of color (transparent) represents that the organism did not form a biofilm under the tested conditions.

Discussion

Based on our results, *A. baumannii* isolates exhibited multidrug resistance, particularly against β-lactam/β-lactamase inhibitors (e.g., piperacillin-tazobactam) and fluoroquinolones (e.g., ciprofloxacin and levofloxacin). Polymyxin B, gentamicin, and aztreonam are more effective options, though resistance is present in some strains. Carbapenems (imipenem and meropenem) remain valuable options but should be cautiously used due to intermediate resistance levels. Resistance patterns emphasize the importance of antimicrobial stewardship to reduce resistance development. Isolates 14 and 9 shared a similar phenotypic pattern, indicating potential resistance to beta-lactams and tetracyclines, and were further studied for biofilm production under different

treatments, including NPs and the supernatant of *L. casei*. Based on the findings of a study, extensively drug-resistant *A. baumannii* strains showed high resistance to antibiotics, including piperacillin-tazobactam and ciprofloxacin, with biofilm-forming ability correlated with increased expression of biofilm-related genes, such as *blaPER-1*, *pgaA*, and *bap* (22). Another study emphasized high resistance to piperacillin-tazobactam, ciprofloxacin, and ceftriaxone among *A. baumannii* isolates, with strong biofilm production identified in more than 50% of strains. However, no direct correlation was observed between antibiotic resistance and biofilm formation (23). Additionally, a study on clinical *A. baumannii* isolates in Taiwan found that many strains were resistant to beta-lactams, including ceftriaxone and ciprofloxacin (24), supporting our finding of resistance to these antibiotics. Our results on the antibacterial effects of the *Lactobacillus* supernatant and Ag NPs against antibiotic-resistant *A. baumannii* (isolates S9 and S14) suggest promising potential for synergistic antimicrobial therapies. Both isolates (S9 and S14) exhibited significant growth reductions, with Ag NPs achieving reductions up to 93.04% (S9) and 88.45% (S14) at 40 mg/µL after 24 hours. This confirms a strong antimicrobial effect, consistent with the known ability of Ag NPs to disrupt bacterial cell walls and membranes, leading to cell death. The supernatant from *Lactobacillus* showed moderate antibacterial effects, with a growth reduction of 70.35% (S9) and 76.45% (S14) at 40 mg/µL after 24 hours. *Lactobacillus* is known for producing antimicrobial substances, such as lactic acid, hydrogen peroxide, and bacteriocins, which could account for these effects. The combination of Ag NPs and the *Lactobacillus* supernatant demonstrated a remarkable synergistic effect, with growth reductions reaching 98.24% (S9) and 90.91% (S14) at 40 mg/µL, implying that the two compounds work together to enhance the antibacterial activity, likely through different but complementary mechanisms, such as the NP-mediated disruption of cell walls and the metabolic interference by the *Lactobacillus* supernatant. Previous studies reported that Ag NPs are effective against multidrug-resistant bacteria, including *A. baumannii*, through mechanisms such as oxidative stress induction and membrane disruption. The combination of Ag NPs and the supernatant of *Lactobacillus* has shown significant synergistic effects against antibiotic-resistant *A. baumannii* isolates S9 and S14. Research indicates that Ag NPs alone can exert potent antibacterial activity against *A. baumannii*, especially against resistant strains. In one study, the combination of Ag NPs with colistin or imipenem displayed synergistic effects, which led to a significant reduction in minimum inhibitory concentration for antibiotics and Ag NPs, enhancing their efficacy against resistant *A. baumannii* strains (25). Ag NPs are also known to inhibit biofilm formation and efflux pumps in *A. baumannii*, contributing to antibiotic resistance. In addition, these NPs have been identified as potent inhibitors of biofilm formation and efflux pumps, making them promising candidates for combating antibiotic-resistant *A. baumannii* (26). The antibacterial and antibiofilm mechanisms of the *L. casei* supernatant and Ag NPs are complex and involve multiple interactions. The bacteriocins produced by *L. casei* disrupt bacterial cell membranes and metabolic functions (27). At the same time, Ag NPs exert their effects by releasing Ag ions, membrane disruption, and reactive oxygen species generation (28). Combining these two agents enhances their individual properties, leading to significantly improved antibacterial and antibiofilm effects, particularly against multidrug-resistant pathogens, such as *A. baumannii*. The vigorous anti-biofilm activity of the Ag NP-supernatant combination highlights its potential as a therapeutic strategy against biofilm-associated infections, especially for resistant pathogens, such as *A. baumannii*. This approach could be instrumental in medical device coatings, wound dressings, or as part of antimicrobial therapies targeting biofilm-forming bacteria.

Conclusion

The combination of Ag NPs and the supernatant had a synergistic effect on inhibiting biofilm formation, making it significantly more effective than either treatment alone. These findings reinforce the potential of combining NPs with biologically active supernatants for combating biofilm-related infections. Further studies can explore the mechanisms behind this synergism and its applicability in clinical or industrial settings.

Acknowledgments

The authors sincerely appreciate the healthcare centers that provided assistance in collecting clinical samples for this study.

Authors' Contribution

Conceptualization: Wisam Talib-Ali, Ashraf Kariminik.
Data curation: Wisam Talib-Ali, Ashraf Kariminik.
Formal analysis: Wisam Talib-Ali, Ashraf Kariminik.
Funding acquisition: Wisam Talib-Ali, Ashraf Kariminik.
Investigation: Wisam Talib-Ali, Ashraf Kariminik.
Methodology: Wisam Talib-Ali.
Project administration: Ashraf Kariminik.
Resources: Wisam Talib-Ali, Ashraf Kariminik.
Software: Atousa Ferdousi.
Supervision: Ashraf Kariminik.
Validation: Ashraf Kariminik, Atousa Ferdousi.
Visualization: Atousa Ferdousi.
Original draft writing: Ashraf Kariminik.
Writing–review & editing: Ashraf Kariminik, Atousa Ferdousi.

Competing Interests

The authors declare that there is no conflict of interests.

Ethical Approval

The Ethics Committee of the Islamic Azad University of Kerman approved this project (IR.IAU.KERMAN.REC.1401.011).

Funding

This study was self-funded by the authors and received no external financial support from any funding organization.

References

1. Ansari H, Tahmasebi-Birgani M, Bijanzadeh M, Doosti A,

Kargar M. Study of the immunogenicity of outer membrane protein A (ompA) gene from *Acinetobacter baumannii* as DNA vaccine candidate in vivo. Iran J Basic Med Sci. 2019;22(6):669-75. doi: 10.22038/ijbms.2019.30799.7427.
2. Hashemzehi R, Doosti A, Kargar M, Jaafarinia M. Cloning and expression of nlpA gene as DNA vaccine candidate against *Acinetobacter baumannii*. Mol Biol Rep. 2018;45(4):395-401. doi: 10.1007/s11033-018-4167-y.
3. Gedefie A, Demsis W, Ashagrie M, Kassa Y, Tesfaye M, Tilahun M, et al. *Acinetobacter baumannii* biofilm formation and its role in disease pathogenesis: a review. Infect Drug Resist. 2021;14:3711-9. doi: 10.2147/idr.S332051.
4. Roy S, Chowdhury G, Mukhopadhyay AK, Dutta S, Basu S. Convergence of biofilm formation and antibiotic resistance in *Acinetobacter baumannii* infection. Front Med (Lausanne). 2022;9:793615. doi: 10.3389/fmed.2022.793615.
5. Kyriakidis I, Vasileiou E, Pana ZD, Tragiannidis A. *Acinetobacter baumannii* antibiotic resistance mechanisms. Pathogens. 2021;10(3):373. doi: 10.3390/pathogens10030373.
6. Vázquez-López R, Solano-Gálvez SG, Juárez Vignon-Whaley JJ, Abello Vaamonde JA, Padró Alonzo LA, Rivera Reséndiz A, et al. *Acinetobacter baumannii* resistance: a real challenge for clinicians. Antibiotics (Basel). 2020;9(4):205. doi: 10.3390/antibiotics9040205.
7. Mea HJ, Yong PVC, Wong EH. An overview of *Acinetobacter baumannii* pathogenesis: motility, adherence and biofilm formation. Microbiol Res. 2021;247:126722. doi: 10.1016/j.micres.2021.126722.
8. Shenkutie AM, Yao MZ, Siu GK, Wong BK, Leung PH. Biofilm-induced antibiotic resistance in clinical *Acinetobacter baumannii* isolates. Antibiotics (Basel). 2020;9(11):817. doi: 10.3390/antibiotics9110817.
9. Maftei NM, Raileanu CR, Balta AA, Ambrose L, Boev M, Marin DB, et al. The potential impact of probiotics on human health: an update on their health-promoting properties. Microorganisms. 2024;12(2):234. doi: 10.3390/microorganisms12020234.
10. Hamad A, Khashan KS, Hadi A. Silver nanoparticles and silver ions as potential antibacterial agents. J Inorg Organomet Polym Mater. 2020;30(12):4811-28. doi: 10.1007/s10904-020-01744-x.
11. Ahmad MA, Aslam S, Mustafa F, Arshad U. Synergistic antibacterial activity of surfactant free Ag-GO nanocomposites. Sci Rep. 2021;11(1):196. doi: 10.1038/s41598-020-80013-w.
12. Amaro F, Morón Á, Díaz S, Martín-González A, Gutiérrez JC. Metallic nanoparticles-friends or foes in the battle against antibiotic-resistant bacteria? Microorganisms. 2021;9(2):364. doi: 10.3390/microorganisms9020364.
13. Abdulrazzak FH, Abed Jawad M, Alkadir OK, Alkaim AF. Antimicrobial activity of Ag:ZnO/MWCNT against *Acinetobacter baumannii*. J Nanostruct. 2021;11(2):317-22. doi: 10.22052/jns.2021.02.012.
14. Al-Shamiri MM, Wang J, Zhang S, Li P, Odhiambo WO, Chen Y, et al. Probiotic *Lactobacillus* species and their biosurfactants eliminate *Acinetobacter baumannii* biofilm in various manners. Microbiol Spectr. 2023;11(2):e0461422. doi: 10.1128/spectrum.04614-22.
15. Mishra MP, Debata NK, Padhy RN. Surveillance of multidrug resistant uropathogenic bacteria in hospitalized patients in Indian. Asian Pac J Trop Biomed. 2013;3(4):315-24. doi: 10.1016/s2221-1691(13)60071-4.
16. Kempf M, Abdissa A, Diatta G, Trape JF, Angelakis E, Mediannikov O, et al. Detection of *Acinetobacter baumannii* in human head and body lice from Ethiopia and identification of new genotypes. Int J Infect Dis. 2012;16(9):e680-3. doi: 10.1016/j.ijid.2012.05.1024.
17. Gupta N, Gandham N, Jadhav S, Mishra RN. Isolation and identification of *Acinetobacter* species with special reference to antibiotic resistance. J Nat Sci Biol Med. 2015;6(1):159-62. doi: 10.4103/0976-9668.149116.
18. Shazadi K, Arshad N. Evaluation of inhibitory and probiotic properties of lactic acid bacteria isolated from vaginal microflora. Folia Microbiol (Praha). 2022;67(3):427-45. doi: 10.1007/s12223-021-00942-5.
19. Syame SM, Mansour AS, Khalaf DD, Ibrahim ES, Gaber ES. Green synthesis of silver nanoparticles using lactic acid bacteria: assessment of antimicrobial activity. Worlds Vet J. 2020;10(4):625-33.
20. Salem WM, Haridy M, Sayed WF, Hassan NH. Antibacterial activity of silver nanoparticles synthesized from latex and leaf extract of *Ficus sycomorus*. Ind Crops Prod. 2014;62:228-34. doi: 10.1016/j.indcrop.2014.08.030.
21. Yang X, Lan W, Xie J. Antimicrobial and anti-biofilm activities of chlorogenic acid grafted chitosan against *Staphylococcus aureus*. Microb Pathog. 2022;173(Pt A):105748. doi: 10.1016/j.micpath.2022.105748.
22. Khosravy M, Hosseini F, Razavi MR, Khavari RA. Expression of biofilm-related genes in extensively drug-resistant *Acinetobacter baumannii*. Jundishapur J Microbiol. 2023;16(4):e133999. doi: 10.5812/jjm-133999.
23. Alamri AM, Alsultan AA, Ansari MA, Alnimr AM. Biofilm-formation in clonally unrelated multidrug-resistant *Acinetobacter baumannii* isolates. Pathogens. 2020;9(8):630. doi: 10.3390/pathogens9080630.
24. Shi ZY, Liu PY, Lau Y, Lin Y, Hu BS, Shir JM. Antimicrobial susceptibility of clinical isolates of *Acinetobacter baumannii*. Diagn Microbiol Infect Dis. 1996;24(2):81-5. doi: 10.1016/0732-8893(96)00017-x.
25. Khaled JM, Alharbi NS, Siddiqi MZ, Alobaidi AS, Nauman K, Alahmedi S, et al. A synergic action of colistin, imipenem, and silver nanoparticles against pandrug-resistant *Acinetobacter baumannii* isolated from patients. J Infect Public Health. 2021;14(11):1679-85. doi: 10.1016/j.jiph.2021.09.015.
26. Shakib P, Saki R, Zolfaghari MR, Goudarzi G. Efflux pump and biofilm inhibitory activity of nanoparticles in *Acinetobacter Baumannii*: a systematic review. Clin Lab. 2023;69(10). doi: 10.7754/Clin.Lab.2023.230227.
27. Al-Dulaimi M, Abdelhameed A, Algburi A. Antimicrobial and anti-biofilm activity of colistin alone and in combination with *Lactobacillus casei* CNCMI 1572 against the clinical isolates of *Acinetobacter baumannii*. Biochem Cell Arch. 2021;21(2):3993-4000.
28. Li X, Gui R, Li J, Huang R, Shang Y, Zhao Q, et al. Novel multifunctional silver nanocomposite serves as a resistance-reversal agent to synergistically combat carbapenem-resistant *Acinetobacter baumannii*. ACS Appl Mater Interfaces. 2021;13(26):30434-57. doi: 10.1021/acsami.1c10309.